Title
A Prospective Study of the Immune System Activation Biomarker Neopterin and Colorectal Cancer Risk

Journal
Journal of the National Cancer Institute, 107(4)

ISSN
0027-8874

Authors
Aleksandrova, Krasimira
Chuang, Shu-Chun
Boeing, Heiner
et al.

Publication Date
2015-04-01

DOI
10.1093/jnci/djv010

JACS
JOURNAL OF THE AMERICAN CHEMICAL SOCIETY

Article

pubs.acs.org/JACS

Observation of Photovoltaic Action from Photoacid-Modified Nafion Due to Light-Driven Ion Transport

William White,[†,§] Christopher D. Sanborn,[†,§] Ronald S. Reiter,[†] David M. Fabian,[†] and Shane Ardo*[,†,‡]

[†]Department of Chemistry and [‡]Department of Chemical Engineering and Materials Science, University of California Irvine, Irvine, California 92697 United States

Supporting Information

ABSTRACT: Replacing passive ion-exchange membranes, like Nafion, with membranes that use light to drive ion transport would allow membranes in photoelectrochemical technologies to serve in an active role. Toward this, we modified perfluorosulfonic acid ionomer membranes with organic pyrenol-based photoacid dyes to sensitize the membranes to visible light and initiate proton transport. Covalent modification of the membranes was achieved by reacting Nafion sulfonyl fluoride poly(perfluorosulfonyl fluoride) membranes with the photoacid 8-hydroxypyrene-1,3,6-tris(2-aminoethylsulfonamide). The modified membranes were strongly colored and maintained a high selectivity for cations over anions. Fourier transform infrared spectroscopy, X-ray photoelectron spectroscopy, and ion-exchange measurements together provided strong evidence of covalent bond formation between the photoacids and the polymer membranes. Visible-light illumination of the photoacid-modified membranes resulted in a maximum power-producing ionic photoresponse of ∼100 μA/cm^2 and ∼1 mV under 40 Suns equivalent excitation with 405 nm light. In comparison, membranes that did not contain photoacids and instead contained ionically associated Ru^{II}–polypyridyl coordination compound dyes, which are not photoacids, exhibited little-to-no photoeffects (∼1 μA/cm^2). These disparate photocurrents, yet similar yields for nonradiative excited-state decay from the photoacids and the Ru^{II} dyes, suggest temperature gradients were not likely the cause of the observed photovoltaic action from photoacid-modified membranes. Moreover, spectral response measurements supported that light absorption by the covalently bound photoacids was required in order to observe photoeffects. These results represent the first demonstration of photovoltaic action from an ion-exchange membrane and offer promise for supplementing the power demands of electrochemical processes with renewable sunlight-driven ion transport.

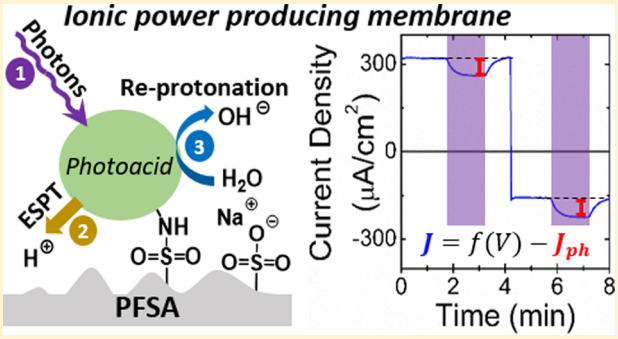

INTRODUCTION

Proton pumps are ubiquitous in biology, where light or adenosine triphosphate drives the proton-pumping process to generate a difference in proton activity across a lipid bilayer.[1,2] When these nonequilibrium conditions are generated using light, the photoconversion process can be termed "photovoltaic" because light is responsible for the generation of a voltage across the membrane.[3−10] When proton transport is accompanied by the transport of other ions to maintain charge neutrality, the energy storage process is chemical like that in batteries, whereas when protons are the only species that are transported, the energy storage process is mostly electric like that in capacitors.[1,2] The most efficient and well-studied solar cells utilize semiconductors with pn-junctions and exhibit photovoltaic action by a capacitive mechanism. We aimed to develop an artificial light-driven proton pump that operated by the same mechanism but with protons and hydroxides serving as the charge-separated species instead of electrons and holes.[10]

Several demonstrations of artificial light-driven proton pumps have been reported.[11−15] Most reports utilized a nanometers-thick lipid bilayer membrane containing molecular dyes, which initiated the proton pumping process by a photoinduced proton-coupled electron-transfer reaction.[4−6,8,9] The report by Bakker and colleagues was unique, because it used a 30 μm thick microporous polyethylene membrane impregnated with merocyanine photoacid dye molecules to sensitize the light-to-ionic energy conversion process.[15] The authors observed a ∼210 mV photovoltage using bidirectional excitation from a Xe arc lamp. This consisted of visible-light illumination from one side of the membrane and ultraviolet-light illumination from the other side of the membrane. Although this proton-pumping process utilized an external optical asymmetry, and not an internal asymmetry like that present in many semiconductors, the magnitude of the photovoltage was independent of the bulk pH, suggesting that the voltage was capacitive, like that observed in state-of-the-art electronic solar cells.

Light absorption by a dye molecule ultimately results in a thermally equilibrated excited state whose electronic and

Received: January 28, 2017
Published: April 17, 2017

DOI: 10.1021/jacs.7b00974
J. Am. Chem. Soc. XXXX, XXX, XXX−XXX

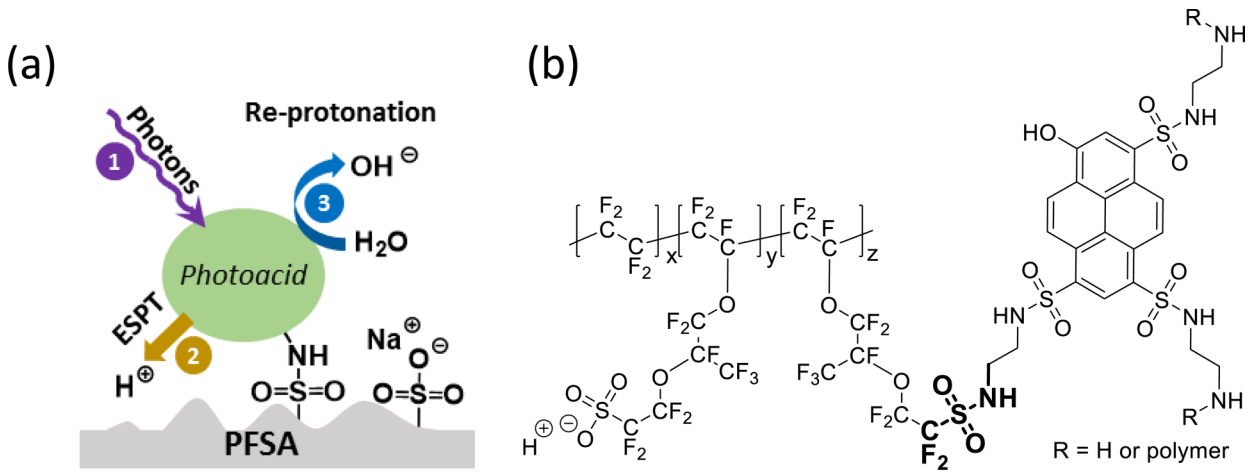

Figure 1. (a) Scheme showing the proposed sensitization cycle of perfluorosulfonic acid ionomer membrane (**PFSA**) modified with 8-hydroxypyrene-1,3,6-tris(2-aminoethylsulfonamide) photoacids, including excited-state proton transfer (ESPT). (b) Proposed structure of the membrane, where R = $-SO_2R'$ or −H. In the case of R = −H, the amine is protonated to form a positively charged ammonium group.

nuclear configurations differ from those of the ground state. In typical dye-sensitized light-to-electrical energy-conversion devices, electron transfer is driven by a change in the redox potential of a dye when it is electronically excited.[16] In our design, proton transfer is driven by a change in the strength of a protic bond of a photoacid dye, and thus its Brønsted acidity, when it is electronically excited (Figure 1a).[17] In aqueous electrolytes at moderate pH, thermodynamically a proton dissociates from the protic group of an excited-state photoacid dye and therefore the concentration of free (or solvated) protons increases, via the reaction PA-OH + photon → $PA\text{-}O^-$ + H^+, where PA-OH is the protonated photoacid molecule. For successful photoacidic dye sensitization, the free proton must cage escape from the conjugate base of the photoacid. Then, in its ground state, the conjugate base of the photoacid is reprotonated by a proton donor, e.g., water, to regenerate the initial state of the photoacid with concomitant formation of the conjugate base of the proton donor, e.g., OH^-.[18−20]

Using this as motivation, we incorporated photoacid dye molecules into Nafion, a perfluorosulfonic acid ionomer membrane (**PFSA**) that is a copolymer with a poly(tetrafluoroethylene) backbone and pendant sulfonate groups attached via perfluorovinyl ether groups.[21] Nafion is the state-of-the-art cation-exchange membrane used in most electrochemical technologies, is completely transparent to visible light, and is a permselective polymer with superb cationic conductivity.[22,23] We intended for Nafion to serve as an optically transparent contact to selectively collect transiently generated protons at the Nafion−solution interface and therefore facilitate photovoltaic action.[10,24] Sensitization of Nafion to visible light was achieved through covalent modification using photoacid dye molecules, 8-hydroxypyrene-1,3,6-tris(2-aminoethylsulfonamide) (Figure 1b), or ionic incorporation of Ru^{II}−polypyridyl coordination compounds. While cationic dye molecules have been incorporated ionically into Nafion for over several decades, covalent modification of Nafion with dye molecules has not been previously reported.[25−28]

EXPERIMENTAL SECTION

Reagents and Chemicals. All chemicals were reagent grade and were used without further purification unless stated otherwise. The following reagents were used as received from the indicated suppliers: sulfuric acid (95%, Fisher Scientific), sodium hydroxide (>95%, Macron Fine Chemicals), Nafion NR-212 poly(perfluorosulfonic acid) membrane (2 mil (50.8 μm) thick, equivalent weight (EW) = 1100, Ion Power), Nafion sulfonyl fluoride poly(perfluorosulfonyl fluoride) membrane (2 mil (50.8 μm) thick, EW = 1100, C.G. Processing), dimethyl sulfoxide (>99.9%, EMD Millipore Corporation), tris(2,2′-bipyridyl)ruthenium(II) chloride hexahydrate (98% Acros Organics), and triethylamine (>99.5%, EMD Millipore Corporation). Purified 8-hydroxypyrene-1,3,6-tris(2-aminoethylsulfonamide), as the trifluoroacetate salt, was available from other work.[29]

Covalent Modification of Nafion Sulfonyl Fluoride Poly(perfluorosulfonyl fluoride) with Hydroxypyrene-Based Photoacid Molecules. First, 3 mg of the trifluoroacetate salt of 8-hydroxypyrene-1,3,6-tris(2-aminoethylsulfonamide) was dissolved in 20 mL of isopropyl alcohol. Then to this solution, 75 μL of 1 M NaOH(aq), 45 μL of triethylamine, and a 2 cm × 2 cm piece of precast Nafion sulfonyl fluoride poly(perfluorosulfonyl fluoride) membrane were added and the reaction was stirred for 7 days at 90 °C, resulting in yellow coloration of the membrane. Inclusion of NaOH ensured that after the synthesis no sulfonyl fluoride groups remained. The membrane was subsequently and serially immersed in 10 mL of the following, for 20 min each: deionized water, 1 M H_2SO_4(aq), 1 M NaOH(aq), deionized water. The membrane was then stored in 1 M NaCl(aq) until use. FTIR−ATR: 627, 981, 1095, 1144, 1200, 1299, 1632, 2857, 2924, 3513, and 3663 cm^{-1}.

Ionic Association of Dye Molecules in Nafion. Freshly cut Nafion membrane (2 cm × 2 cm) was pretreated by stirring in 1 M H_2SO_4(aq) for 1 h. A stock solution of the photoacid dye 8-hydroxypyrene-1,3,6-tris(2-aminoethylsulfonamide) was prepared by dissolving 20 mg of photoacid in 10 mL of 1 M H_2SO_4(aq) to a final concentration of 3.4 mM. A stock solution of the dye $[Ru(bpy)_3]Cl_2$ was prepared by dissolving 25 mg of $[Ru(bpy)_3]Cl_2{\cdot}6H_2O$ in 20 mL of 1 M H_2SO_4(aq) to a final concentration of 1.6 mM, where bpy is 2,2′-bipyridine. For each dye, 5 mL of dye stock solution was added to a scintillation vial along with a 2 cm × 2 cm piece of precast Nafion and stirred for 36 h at 80 °C.

Ion Exchange Capacity. Membranes were dried for 24 h at 80 °C under reduced pressure, and a dry weight was measured gravimetrically. The membranes were then rinsed with copious amounts of deionized water and then immersed in 20 mL of 1 M HCl(aq) and stirred for 24 h at room temperature. The protonated films were then rinsed with copious amounts of deionized water, immersed in 1 M NaCl(aq), and stirred for 24 h at room temperature. The membranes were then removed, and the soaking solution was titrated to pH 7 using 10 mM NaOH(aq). Ion exchange capacity (mmol g^{-1}) was calculated as the volume (L) of 10 mM NaOH(aq) used to titrate the

DOI: 10.1021/jacs.7b00974
J. Am. Chem. Soc. XXXX, XXX, XXX−XXX

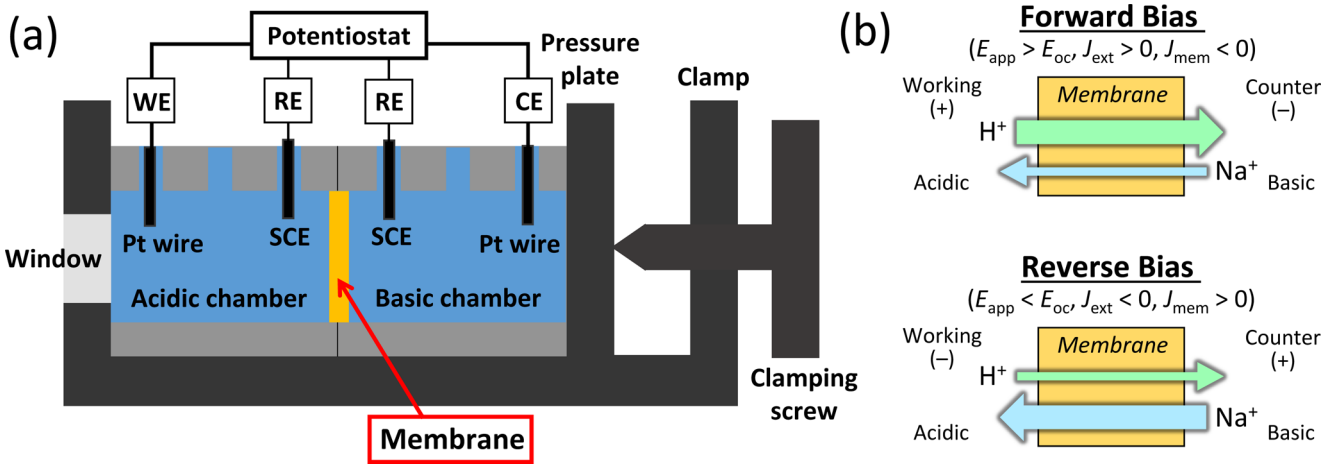

Figure 2. (a) Electrochemical cell used to conduct photoelectrochemical experiments indicating the locations of the working electrode (WE), counter electrode (CE), and reference electrodes (REs) with respect to the locations of the ion-exchange membrane, the acidic and basic electrolytes, and the borosilicate glass window. (b) Conditions during forward bias (top) and reverse bias (bottom) of the electrochemical cell including the polarization of the working/acidic compartment versus the counter/basic compartment, the sign of the applied bias (E_{app}) versus the open-circuit potential in the dark (E_{oc}), the sign of the current density at the WE through the potentiostat (J_{ext}) and through the membrane (J_{mem}) (and where all current densities reported herein are J_{ext} values), and the predominant ions responsible for current in the electrolyte, with arrow sizes that are qualitatively proportional to expected transport numbers.

solution to pH 7 multiplied by its concentration (10 mM) and divided by the dry mass of each membrane (g).[30,31]

Ultraviolet–Visible (UV–Vis) Electronic Absorption Spectroscopy. Electronic absorption spectra were acquired at room temperature using a UV–Vis spectrophotometer (Cary 60, Agilent Technologies) with a resolution of 1 nm. UV–Vis absorption spectra were measured by mounting membranes in the beam path, and spectra are reported versus a baseline spectrum taken on ambient air and after correction for the nonzero absorption at 750 nm due to scattering by subtracting the observed absorbance value at 750 nm from all data points in the spectrum.

Infrared Spectroscopy. Membranes were dried for >24 h at 105 °C and under reduced pressure prior to measurements. Fourier transform infrared spectroscopy in attenuated total reflectance (ATR) detection mode was performed on a Jasco FT/IR-4700 spectrophotometer equipped with a monolithic diamond ATR crystal. Spectra were acquired with a resolution of 1 cm^{-1} and an acquisition time of 74 s, and spectra are reported versus a baseline spectrum taken on ambient air.

X-ray Photoelectron Spectroscopy. Membranes were dried for >2 h at room temperature and under reduced pressure prior to measurements. X-ray photoelectron spectroscopy was performed using an AXIS Supra by Kratos Analytical with an Al Kα X-ray source (1486.8 eV). Survey scans were taken first, followed by high-resolution scans of each element region. The raw data was shifted to higher binding energies so that the C 1s binding energy for an sp^3 hybridized R–CF_2–R′ group corresponded to the literature value of 292.2 eV.[32]

Fluorescence Microscopy. A custom-built two-photon excitation microscope based on an Olympus FV1000 microscope (Olympus Corporation, Tokyo, Japan) was used for solution lifetime measurements. Photoacid dye was dissolved in either concentrated 12 M HCl(aq) or dissolved in aqueous buffered solution and titrated to pH 8. The microscope was equipped with an Olympus 60X UPlanAPO objective (numerical aperture of 1.2, water immersion) (Olympus Corporation, Tokyo, Japan). Multiphoton excitation was achieved using a mode-locked 80 MHz Ti:sapphire laser (Chameleon Ultra, Coherent Inc., Santa Clara, CA) tunable from 690 to 1040 nm. The laser power was controlled by an acoustic optical modulator, and the signal was detected using a two-channel detection unit with two photosensor modules (H7422P-40, Hamamatsu Photonics KK). The fluorescence signal collected by the detectors was externally amplified and fed to a constant fraction discriminator (model 6915, Phillips Scientific, Mahwah, NJ) to produce TTL signals. These TTL pulses were counted using a Fast FLIM box (A320, ISS, Champaign, IL) and registered based on the arrival time and phase with respect to the excitation laser pulse. The channels were separated with a dichroic unit: channel 1, 460/50 nm, and channel 2, 525/50 nm. All data was obtained and analyzed using Sim-FCS software (Laboratory for Fluorescence Dynamics, UCI, http://www.lfd.uci.edu/globals/, Irvine, CA).

For cross-sectional fluorescence imaging, membranes were freshly cut using a razor blade, placed between two glass microscope slide supports, and oriented with their large areas parallel to the direction of propagation of the incident light output from a user-modified Olympus FV1000 microscope (Olympus Corporation, Tokyo, Japan). Electrolyte (10 mM HCl(aq)) was introduced to the membrane via capillary action by placing a drop between the edges of the microscope slides. An Ar-ion laser (LASOS Lasertechnik GmbH, Jena, Germany) with an acoustic optic tunable filter enabled 488 nm excitation. Cross sections were imaged at 1024 × 1024 pixels with a pixel dwell time of 10 μs and a pixel size of 210 nm. The data was processed using ImageJ to plot mean cross-sectional intensity profiles across the film thickness.

Photoelectrochemical Procedures. Platinum electrodes were fabricated by soldering a platinum wire (1 cm long, 300 μm diameter) to a piece of insulated tinned Cu wire and inserting and sealing this into a glass tube using two-part epoxy (Loctite Hysol 1C). Platinum electrodes were used as the power/current-carrying electrodes and were placed on opposite sides of the membrane, with the working electrode (WE) in the acidic chamber and the counter electrode (CE) in the basic chamber. Nominally identical saturated calomel electrodes (SCEs, KCl saturated) (CH Instruments, Inc.) served as the reference electrodes (REs) and were placed on opposite sides of the membrane to measure the potential difference across it. The electrochemical cell (Figure 2a) consisted of two poly(chlorotrifluoroethylene) blocks, each containing a horizontal cylindrical channel with a diameter of 1.54 cm and three vertical cylindrical holes on the top of each block, each 0.5 cm in diameter and spaced 1 cm apart center-to-center. The electrochemical cell was connected to a potentiostat (VSP-300, Bio-Logic), with the two current-carrying leads attached to the platinum electrodes and the two potential-sensing leads attached to the reference electrodes. Reported current densities were calculated by dividing the external current passed through the potentiostat by the geometric area of the membrane exposed to the aqueous electrolyte solution (1.86 cm^2). A negative external current meant that net electrons moved from the Pt wire CE through the external circuit to

DOI: 10.1021/jacs.7b00974
J. Am. Chem. Soc. XXXX, XXX, XXX–XXX

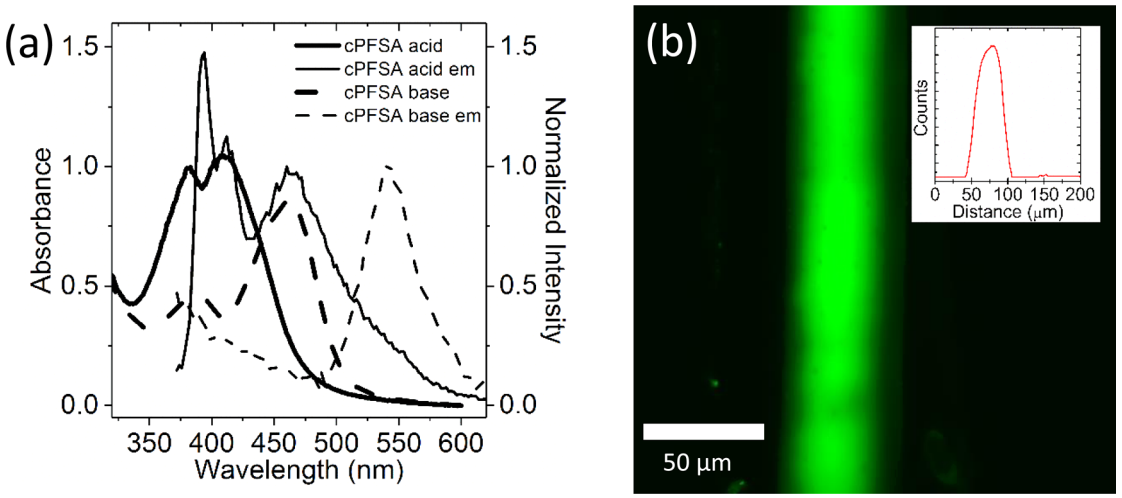

Figure 3. (a) Electronic absorption (solid lines) and emission (dashed lines) spectra of **cPFSA** after protonation by strong acid (1 M H_2SO_4(aq); bold lines) or deprotonation by strong base (1 M NaOH(aq); thin lines). (b) Cross sectional fluorescence microscopy image of **cPFSA** with the inset depicting the fluorescence intensity versus position.

the Pt wire WE and therefore that there was a positive membrane current, where cations in the electrolyte moved toward the Pt wire WE from the basic chamber to the acidic chamber and/or that anions moved in the opposite direction, as shown in Figure 2b. In the dark, this process occurred under reverse-bias conditions when the applied bias was less than the so-called open-circuit potential (E_{oc}). Open-circuit potentials were measured using galvanostatic chronopotentiometry performed at 0 μA. Current densities (J) at each potential (E) were measured using potentiostatic chronoamperometry. Rate constants were determined by fitting the rise and the fall for each of the photovoltage and photocurrent transients to a single exponential function ($y = A \exp[-t/\tau] + B$, with fitted parameters of A, τ, and B).

All electrochemical data was corrected for baseline drift using a linear−exponential combination fit ($y = at + b \exp[ct + d]$, with fitted parameters of a, b, c, and d) of the data in the dark before illumination started and after illumination ceased. This baseline correction was performed in order to deconvolute the photoresponse from the background drift because E_{oc} changed slightly over the course of the experiment due to reduction of the junction potential through exchange of Na^+ and H^+ across the cation-exchange membrane.

Optical excitation was achieved using continuous-wave light from laser pointers that emitted at 405 ± 10 nm (fwhm = 1.96 mm; (1 ± 0.2) × 10^{18} photon cm^{-2} s^{-1}), 532 ± 10 nm (fwhm = 0.96 mm; (6.47 ± 2) × 10^{18} photon cm^{-2} s^{-1}), or 650 ± 10 nm (fwhm = 1.91 mm; (1.1 ± 0.4) × 10^{19} photon cm^{-2} s^{-1}). Each was calibrated using a knife-edge measurement and a silicon photodiode detector (FDS100, Thorlabs). Briefly, a razor blade was affixed to a micrometer stage, and photocurrent was measured on the silicon detector as a function of the transverse position of the blade; the absence of a blade was used to calculate the total photon flux. The derivative of the resulting sigmoidal best-fit functions to the light intensity versus blade position were Gaussian functions whose maximum value was used to determine the full width at half-maximum of the collimated illumination, which was used as the dimension in calculating the approximate square illumination area. The absorbed photon fluence rate at 405 nm was calculated by multiplying the photon fluence rate at 405 nm by the absorptance of the sample at the 405 nm excitation wavelength ($1-10^{-Abs405}$). This absorbed photon fluence rate was then converted into an equivalent number of Suns excitation by dividing it by the absorbed photon fluence rate expected under conditions of excitation by 1 Sun of Air Mass 1.5 Global solar illumination. Using the absorption spectrum of **PFSA** containing covalently bound photoacids (**cPFSA**) at wavelengths less than 550 nm, the equivalent number of Suns excitation was determined to be 40.

Turnover numbers were calculated from light-generated current density (J_{ph}) values measured from 177 consecutive cycles of 30 min of illumination using 405 nm light followed by 30 min of darkness. For these measurements, the photoactive area was reduced to 0.237 cm^2 using a Viton sheet to cover the majority of the membrane from being wetted by electrolyte. Electrolyte was refreshed every 24 h.

RESULTS AND DISCUSSION

Polymer Materials Synthesis and Characterization. Covalently modified **PFSA** (**cPFSA**) was synthesized by immersing precast Nafion sulfonyl fluoride poly(perfluorosulfonyl fluoride) membrane (**PFSF**) in an isopropyl alcohol and water mixture containing the photoacid, triethylamine, and NaOH. Electronic absorption spectra of **cPFSA** in both the protonated and deprotonated forms (Figure 3a) are consistent with spectra of the photoacids dissolved in aqueous solution (Supporting Information, Figure S1). Deprotonation resulted in a 0.35 eV bathochromic shift of the lowest-energy absorption transition. Cross-sectional photoluminescence microscopy images of **cPFSA** indicated that photoacids were present throughout the ∼50 μm thickness of the membrane and that the near-surface regions contained fewer photoacids than in the bulk (Figure 3b).

Covalent bonding of photoacids in **cPFSA** were supported by data shown in Figure 4, which contains the Fourier transform infrared (FTIR) spectra and X-ray photoelectron spectroscopy (XPS) spectra for Nafion, **PFSF**, **cPFSA**, and ionomer membranes containing ionically associated photoacids (**iPFSA**). The characteristic sulfonyl fluoride peaks at 795, 823, and 1467 cm^{-1} present in FTIR spectra of **PFSF** were undetectable in spectra of **cPFSA**, which was synthesized from **PFSF**.[33−36] This suggests that most sulfonyl fluoride groups were modified to sulfonates/sulfonic acids or covalently bound dyes in **cPFSA**.[36−41] Two small peaks were also present in the 2800−2950 cm^{-1} range for **iPFSA** and **cPFSA**, which based on previous literature reports are consistent with assignment to C−H stretches in the pyrene core of the photoacids (Supporting Information, Figures S2 and S3).[42] Partial hydration of the membranes precluded accurate identification of sulfonate and sulfonamide vibrational modes due to overlap with strong and broad vibrational peaks at 1625 and 3530 cm^{-1}, which are characteristic of water in hydrated Nafion.[36,38,41]

To learn more about the binding of the photoacids in **PSFA**, the four samples were analyzed using XPS over the range of

DOI: 10.1021/jacs.7b00974
J. Am. Chem. Soc. XXXX, XXX, XXX−XXX

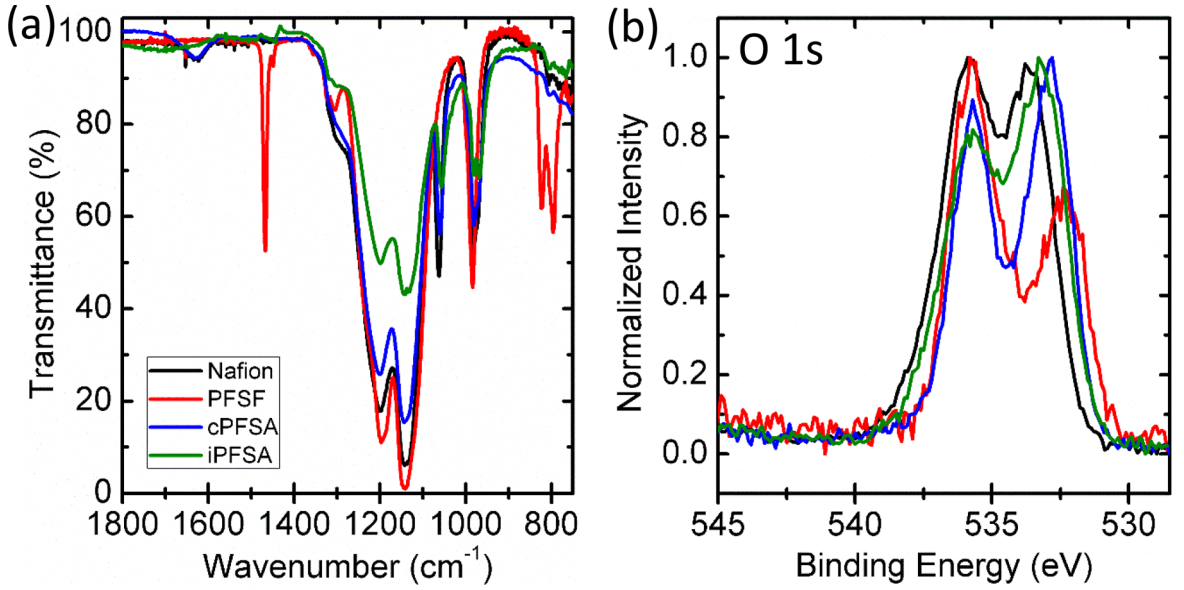

Figure 4. (a) Low-energy FTIR–ATR transmission spectra and (b) O 1s XPS spectra for Nafion (black), **PFSF** (red), **cPFSA** (blue), and **iPFSA** (green), with each spectrum normalized to its largest intensity peak. The key in (a) is also accurate for the data in (b).

energies for core emission from O (Figure 4b) and C, N, F, and S (Supporting Information, Figure S4). The O 1s core region spectra are diagnostic of the substitution of sulfonyl fluoride and clearly show a difference in binding energy between the mixed sulfonamide/sulfonate-containing membranes (**cPFSA** and **iPFSA**) and the sulfonate-only-containing membrane, Nafion. Prior literature supports that the higher binding energy peak at >535 eV is attributed to the ether oxygen atoms in the polymer and that the lower binding energy peak at 531–534 eV is attributed to the sulfonyl oxygen atoms.[38,43–45] The binding energies of oxygen bound to sulfur exhibit a logical trend, SO_3^- > SO_2NR, based on the convolution of electronegativity and electron donating strength of the substituents.[44] This trend is observed between **cPFSA** and **iPFSA**, where the smaller binding energy observed for **cPFSA** is consistent with it having a greater proportion of sulfonamides, due to the formation of covalent membrane–photoacid sulfonamide bonds, as compared to **iPFSA**, which only has sulfonamide bonds in the photoacid structure itself.

When **cPFSA** was immersed in 1 M NaOH(aq) for 2 h, there was no visual evidence for leaching of dyes into solution. Conversely, when **iPFSA** was submerged in the same electrolyte, desorption of dyes was immediately apparent. Together, the FTIR and XPS spectroscopy results and alkaline ion-exchange studies suggest that photoacids reacted with the sulfonyl fluoride groups in **PFSF** and resulted in covalent modification as **cPFSA**.

The membranes were also found to be mechanically robust and chemically stable. Submerging **cPFSA** in water, *N*,*N*-dimethyl-formamide, or dimethyl sulfoxide for 7 days at 100 °C resulted in no apparent dissolution of the membrane suggesting that the polymer may be cross-linked. The average ion-exchange capacity for **cPFSA** was determined to be 0.66 ± 0.06 mequiv/g, while Nafion was measured to have an ion-exchange capacity of 0.83 ± 0.07 mequiv/g,[46] indicating that the ion-exchange capacity changed by > ~5%, as 1 − ((0.66 + 0.06)/(0.83 − 0.07)). Synthesis of **cPFSA** used 60 mg of **PFSF** (~55 μmol of sulfonyl fluoride groups) and 3.2 μmol of photoacid. Given that the ion-exchange capacity technique identifies protons associated with sulfonates and protons present in the alcohol group of the photoacids, bonding each photoacid molecule to the polymer via one sulfonamide does not change the measured ion-exchange capacity. The most likely scenario is that each photoacid molecule bonded to the polymer via two sulfonamides, therefore replacing two sulfonate protons with one alcohol proton in the ion-exchange capacity measurement and decreasing the ion-exchange capacity by ~6%, as (3.2/55). However, this assumes no cross-linking of **cPFSA** by the photoacids, which may render some of the sulfonates inaccessible to electrolyte. The FTIR spectra of **cPFSA** and **iPSFA** do not exhibit clear peaks that are characteristic of the photoacid as a powder, making it difficult to assign the binding mode of the photoacid (Supporting Information, Figure S3).

Assessment of Photoelectrochemical Performance. For **cPFSA** to exhibit photovoltaic action, i.e., a photovoltage and power production when illuminated, it must absorb light, separate charge, and collect charge.[10] Electronic absorption spectra suggest that protonated photoacids in **cPFSA** absorb visible light. Photoluminescence data exhibiting a shoulder at ~550 nm indicate some radiative decay from specifically *deprotonated* excited-state photoacids in **cPFSA** (Figure 3), supporting the assignment of this process to charge separation by excited-state proton transfer. A measurable photovoltage response under open-circuit conditions suggests that both charge separation *and* cage escape of photoliberated protons from the solvation environment of the photoacids occurred (Figure 5a). Charge collection was verified by measurements of the photocurrent densities (Figure 5b). Observation of a nearly constant steady-state photocurrent from electronically insulating **cPFSA** supported that illumination resulted in an increase in the rate of ion transport to the current-carrying electrodes of the potentiostat.[47]

The steady-state open-circuit potential across the membrane *in the dark*, E_{oc}, was measured to be approximately −30 mV. This is ascribed to a liquid-junction electric potential generated by the difference in the concentration of protons and Na^+ across the membrane.[48] The negative sign of E_{oc} is consistent with proton diffusion from the acidic to the alkaline electrolyte

DOI: 10.1021/jacs.7b00974
J. Am. Chem. Soc. XXXX, XXX, XXX–XXX

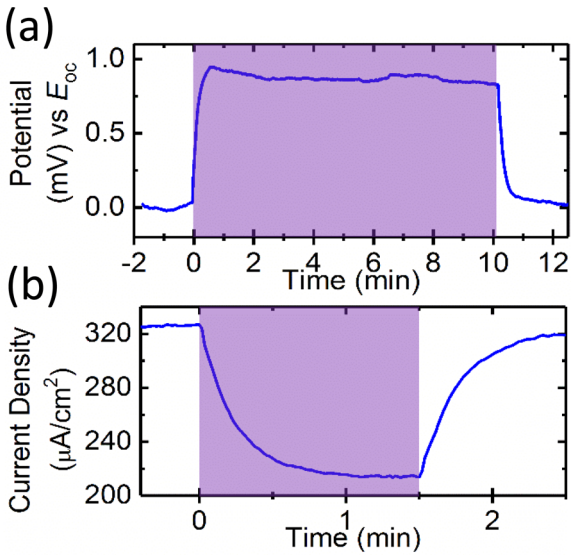

Figure 5. (a) Open-circuit photovoltage and (b) photocurrent at a small positive bias for **cPFSA** wetted by 1 M H_2SO_4(aq) on one side of the membrane and 1 M NaOH(aq) on the other side of the membrane. Regions highlighted in purple indicate illumination with 405 nm laser light at 40 Suns equivalent excitation.

that is faster than Na^+ diffusion in the opposite direction.[49] The open-circuit photovoltage *in the light versus* E_{oc} was measured to be approximately +1 mV. The positive sign of the photovoltage means that illumination decreased the magnitude of the electric potential across the membrane, behavior that is consistent with the conclusion that the membrane exhibited photovoltaic action. The *steady-state* liquid-junction electric potential in the dark and observation of photovoltaic action are analogous to conditions in traditional semiconductor pn-junction and Schottky-junction solar cells, except that *equilibration* in the dark generates the built-in electric potential in a traditional semiconductor. In the presence of inert or acidic electrolyte at the same concentration on both sides of Nafion, an electric potential difference was not measured and photovoltaic action was not observed.

While the photovoltaic properties observed for **cPFSA** are poor, pathways to larger efficiencies do exist. For example, assuming that the concentration of photoacids in **cPFSA** was increased to the concentration of sulfonate groups in Nafion, the photocurrent observed herein would be expected under conditions of ~10 times less intense illumination. Moreover, use of a bipolar membrane structure instead of a single monopolar ion-exchange membrane would likely slow ion leakage and generate much larger built-in potentials.[48] This would conceivably result in larger photovoltages and therefore larger light-to-ionic energy conversion efficiencies.

The rise and decay of the photocurrent (τ_{rise} = 16 s and τ_{fall} = 14 s) and the photovoltage (τ_{rise} = 10 s and τ_{fall} = 10 s) signals were each well described by an exponential process (Supporting Information, Figure S5). The similarity of the rates of all four processes suggests that the current transients were due to capacitive charging and/or attaining a steady-state mass-transport regime.[49] To further assess the photophysical and photochemical properties of the photoacid, the quantum yield of emission, ϕ_{em} (~0.29), and rate constants for excited-state deactivation, k_r and k_{nr}, were calculated for photoacids dissolved in acidic aqueous solution (Supporting Information, Table S2). Increasing ϕ_{em} for photoacids bound to **cPFSA** may be important for attaining large photovoltages because the ultimate efficiency limit for photovoltaic devices occurs when the rate-determining recombination process is radiative decay of the excited state, and therefore ϕ_{em} = 1.[50]

Measurements of the power-producing region of *J*–*E* behavior in the light were imperfect due to the weak photoresponses and difficulties in generating a stable short-

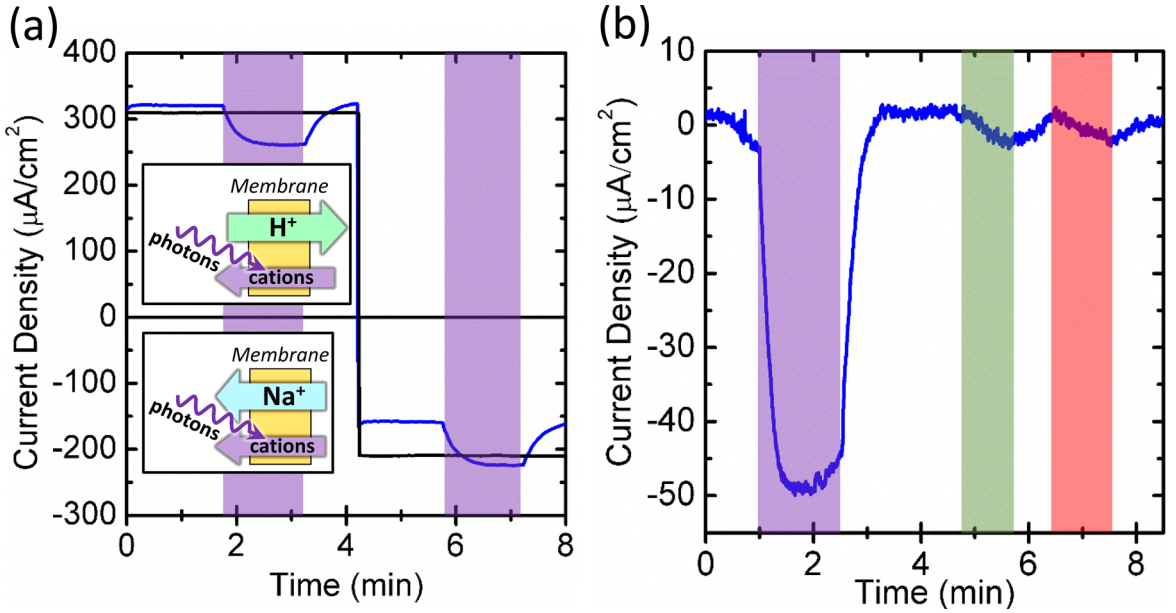

Figure 6. Chronoamperometry data in the dark and under illumination (highlighted regions) for **cPFSA** (blue) wetted by 1 M H_2SO_4(aq) on one side and 1 M NaOH(aq) on the other side of the membrane. (a) Data measured under forward bias (left, and top inset) and reverse bias (right, and bottom inset) and for Nafion impregnated with $Ru(bpy)_3^{2+}$ (black), under the same conditions. (b) Spectral response, reported as J_{ph} values after correction for a dark current density of 1.4 ± 0.6 μA/cm², when illuminated with laser light at 405 nm (purple), 532 nm (green), and 650 nm (red), colored, respectively.

DOI: 10.1021/jacs.7b00974
J. Am. Chem. Soc. XXXX, XXX, XXX–XXX

circuit condition, i.e., applying a bias precisely equal to E_{oc}. However, additional chronoamperometry measurements supported the conclusion that **cPFSA** exhibited photovoltaic action because the sign of J_{ph}, calculated as the difference in the light versus dark current densities, was independent of the sign of the applied potential (Figure 5b and Figure 6). For a solar cell, J_{ph} is the contribution to the current that results from optical excitation, and in the ideal case it is a constant value irrespective of potential bias.[10,24] In practice, this value is at least single-signed over the power-producing region, behavior that was observed for **cPFSA** in this region and beyond (Supporting Information, Figure S6).

Diagrams of the membrane under forward bias or reverse bias conditions are shown as insets to Figure 6a, with clear indication of the expected type and direction of majority cation flux. While these fluxes have not been measured directly, precedent from related Nafion membranes supports that these processes are likely occurring. Given the experimental setup, a negative value for J_{ph} is consistent with light driving net *cation* transport into the compartment with a large concentration of protons. Because the dyes are photoacids, our hypothesis is that the observed behavior is specifically due to light-driven *proton* transport against a pH gradient, behavior that is consistent with photovoltaic action.

The previous data do not preclude that thermal effects from local heating were at least in part responsible for the observed behavior. Nafion has been shown to have a Seebeck coefficient that depends on the relative humidity, bias, and/or temperature.[51] For relative humidities >50%, the Seebeck coefficient was observed to be negative, with a reported maximum magnitude value of −2 mV/K. This implies that increasing the local temperature could result in behavior consistent with photovoltaic action. Therefore, a comparison was made between **cPFSA** and Nafion containing ionically associated $Ru(bpy)_3^{2+}$ dyes, **iPFSA-Ru** (Figure 6a). $Ru(bpy)_3^{2+}$ dissolved in aqueous solution exhibits a large nonradiative rate constant and a quantum yield of emission that is smaller than that observed for the photoacids dissolved in aqueous solution (ϕ_{em} < 0.07 for $Ru(bpy)_3^{2+}$ and $\phi_{em} \approx 0.29$ for the photoacid).[52] Notwithstanding, J_{ph} values for **cPFSA** were observed to be orders-of-magnitude larger than for **iPFSA-Ru**, which implies that the observed photovoltaic action for **cPFSA** was not due to local heating caused by nonradiative decay of the excited-state photoacids or electron-transfer/energy-transfer to dissolved O_2 in the aqueous electrolyte.

The photocurrent response of **cPFSA** was over an order-of-magnitude larger when illuminated with 405 nm light in comparison to illumination with 532 or 650 nm light, whose photon fluxes were each more than six times larger (Figure 6b). This further supports the conclusion that photovoltaic action was due to optical excitation of the photoacids and not due to other optical effects. Also, over the course of a 177-hr experiment, the total number of charges passed was calculated to be 3.55 μmol. Given that the maximum concentration of dyes within the entire 4 cm^2 film was 3.2 μmol, and that the membrane area in direct contact with the electrolyte and illuminated was 0.237 cm^2, the photoacids exhibited a turnover number of >18 and the photocurrent response was stable over the course of the experiment, meaning the sensitization process was regenerative/photocatalytic and not stoichiometric.

CONCLUSIONS

Using **PFSA** modified with photoacid dye molecules, 8-hydroxypyrene-1,3,6-tris(2-aminoethylsulfonamide), a first-of-its-kind synthetic polymer membrane light-driven proton pump was demonstrated. Bonding of photoacids to the polymer was supported by results obtained using FTIR−ATR spectroscopy and XPS, and clear differences in the transport of ionically associated dyes when in contact with strongly alkaline aqueous electrolyte. **cPFSA** was shown to undergo excited-state proton transfer and exhibited photovoltaic action with a turnover number of >18. Maximum photoresponses were $J_{ph} \approx 100$ μA/cm^2 and ∼1 mV open-circuit photovoltage under 40 Suns equivalent excitation with 405 nm light. This behavior was clearly different (at least an order-of-magnitude larger J_{ph}) than that observed for Nafion that contained ionically associated $Ru(bpy)_3^{2+}$ dyes or **cPFSA** illuminated with 532 or 650 nm light. This new class of dye-sensitized ion-exchange materials is capable of alleviating power demands from electrochemical processes such as electrodialysis and electrolytic generation of acid and base.

ASSOCIATED CONTENT

Supporting Information

The Supporting Information is available free of charge on the ACS Publications website at DOI: 10.1021/jacs.7b00974.

Additional electronic absorption spectra, additional FTIR−ATR spectra, additional XPS core region spectra, kinetics of photocurrent and photovoltage generation, J_{ph}−E behavior, procedure and results for determination of the quantum yield of emission (PDF)

AUTHOR INFORMATION

Corresponding Author

*ardo@uci.edu

ORCID

Shane Ardo: 0000-0001-7162-6826

Author Contributions

[§]W.W. and C.D.S. contributed equally to this work.

Notes

The authors declare no competing financial interest.

ACKNOWLEDGMENTS

We are grateful for financial support from the Department of Chemistry and the School of Physical Sciences at the University of California Irvine and the Gordon and Betty Moore Foundation via a Moore Inventor Fellowship under Grant #5641. R.S.R. was supported by a UC Irvine Chancellor's Fellowship. D.M.F. is supported by a National Science Foundation Graduate Research Fellowship under Grant No. DGE-1321846. We thank Lee Moritz from the UC Irvine Machine Shop and Rick P. Gerhart from the Caltech Glassblowing Shop for fabricating custom electrochemical cells, Prof. Enrico Gratton and Prof. Michelle Digman for use of their Laboratory of Fluorescence Dynamics (LFD) and Dr. Jenu Varghese Chacko for training and assistance with the laser microscopy instruments in the LFD, and Dr. Walter Grot for advice and for generously supplying Nafion sulfonyl fluoride poly(perfluorosulfonyl fluoride) membrane and ionic dyes for use in permselectivity experiments. FTIR and photoluminescence experiments were performed at the UCI Laser Spectroscopy Facility under the supervision of the Facility Director, Dr.

DOI: 10.1021/jacs.7b00974
J. Am. Chem. Soc. XXXX, XXX, XXX−XXX

Dima Fishman. XPS experiments were performed at the UC Irvine Materials Research Institute (IMRI) using instrumentation funded in part by the National Science Foundation Major Research Instrumentation Program under grant no. CHE-1338173. We thank Dr. Ich Tran for guidance in XPS data analysis.

REFERENCES

(1) Nelson, D. L.; Cox, M. M. *Lehninger Principles of Biochemistry*, 6th ed.; W. H. Freeman: New York, 2012.
(2) Skulachev, V. P.; Bogachev, A. V.; Kasparinsky, F. O. *Principles of Bioenergetics*; Springer Science & Business Media: Berlin, 2012.
(3) Bard, A. J.; Memming, R.; Miller, B. *Pure Appl. Chem.* **1991**, *63*, 569−596.
(4) Singh, K.; Korenstein, R.; Lebedeva, H.; Caplan, S. R. *Biophys. J.* **1980**, *31*, 393−401.
(5) Eisenbach, M.; Weissmann, C.; Tanny, G.; Caplan, S. R. *FEBS Lett.* **1977**, *81*, 77−80.
(6) Chu, L.; Yen, C.; El-Sayed, M. A. *Biosens. Bioelectron.* **2010**, *26*, 620−626.
(7) Gust, D.; Moore, T. A.; Moore, A. L. *Acc. Chem. Res.* **2001**, *34*, 40−48.
(8) Liddell, P. A.; Kuciauskas, D.; Sumida, J. P.; Nash, B.; Nguyen, D.; Moore, A. L.; Moore, T. A.; Gust, D. *J. Am. Chem. Soc.* **1997**, *119*, 1400−1405.
(9) Moore, T. A.; Gust, D.; Mathis, P.; Mialocq, J.-C.; Chachaty, C.; Bensasson, R. V.; Land, E. J.; Doizi, D.; Liddell, P. A.; Lehman, W. R.; Nemeth, G. A.; Moore, A. L. *Nature* **1984**, *307*, 630−632.
(10) Fonash, S. *Solar Cell Device Physics*; 2nd ed.; Elsevier: Burlington, MA, 2010.
(11) Sun, K.; Mauzerall, D. *Proc. Natl. Acad. Sci. U. S. A.* **1996**, *93*, 10758−10762.
(12) Steinberg-Yfrach, G.; Liddell, P. A.; Hung, S.-C.; Moore, A. L.; Gust, D.; Moore, T. A. *Nature* **1997**, *385*, 239−241.
(13) Tributsch, H. *Ionics* **2000**, *6*, 161−171.
(14) Bhosale, S.; Sisson, A. L.; Talukdar, P.; Fürstenberg, A.; Banerji, N.; Vauthey, E.; Bollot, G.; Mareda, J.; Röger, C.; Würthner, F.; Sakai, N.; Matile, S. *Science* **2006**, *313*, 84−86.
(15) Xie, X.; Crespo, G. A.; Mistlberger, G.; Bakker, E. *Nat. Chem.* **2014**, *6*, 202−207.
(16) Ardo, S.; Meyer, G. J. *Chem. Soc. Rev.* **2009**, *38*, 115−164.
(17) Spry, D. B.; Fayer, M. D. *J. Chem. Phys.* **2008**, *128*, 084508.
(18) Donten, M. L.; Hamm, P.; VandeVondele, J. *J. Phys. Chem. B* **2011**, *115*, 1075−1083.
(19) Natzle, W. C.; Moore, C. B. *J. Phys. Chem.* **1985**, *89*, 2605−2612.
(20) Henrich, J. D.; Suchyta, S.; Kohler, B. *J. Phys. Chem. B* **2015**, *119*, 2737−2748.
(21) Gaieck, W.; Ardo, S. *Reviews in Advanced Sciences and Engineering* **2014**, *3*, 277−287.
(22) Banerjee, S.; Curtin, D. E. *J. Fluorine Chem.* **2004**, *125*, 1211−1216.
(23) Mauritz, K. A.; Moore, R. B. *Chem. Rev.* **2004**, *104*, 4535−4585.
(24) Würfel, P. *Physics of Solar Cells: From Principles to New Concepts*; Wiley-VCH: Weinheim, Germany, 2005.
(25) Abraham John, S.; Ramaraj, R. *J. Electroanal. Chem.* **2004**, *561*, 119−126.
(26) John, S. A.; Ramaraj, R. *Langmuir* **1996**, *12*, 5689−5695.
(27) García-Fresnadillo, D.; Marazuela, M. D.; Moreno-Bondi, M. C.; Orellana, G. *Langmuir* **1999**, *15*, 6451−6459.
(28) Sabatani, E.; Nikol, H. D.; Gray, H. B.; Anson, F. C. *J. Am. Chem. Soc.* **1996**, *118*, 1158−1163.
(29) Sanborn, C. D.; Chacko, J. V.; Ardo, S. *in preparation*.
(30) Chen, T. Y.; Leddy, J. *Langmuir* **2000**, *16*, 2866−2871.
(31) Ma, L.; Li, J.; Xu, G.; Xiong, J.; Cai, W. *RSC Adv.* **2016**, *6*, 114899−114905.
(32) Schulze, M.; Lorenz, M.; Wagner, N.; Gülzow, E. *Fresenius' J. Anal. Chem.* **1999**, *365*, 106−113.
(33) Greso, A. J.; Moore, R. B.; Cable, K. M.; Jarrett, W. L.; Mauritz, K. A. *Polymer* **1997**, *38*, 1345−1356.
(34) Gruger, A.; Régis, A.; Schmatko, T.; Colomban, P. *Vib. Spectrosc.* **2001**, *26*, 215−225.
(35) Perusich, S. A. *J. Appl. Polym. Sci.* **2011**, *120*, 165−183.
(36) Hillman, D. M.; Stephens, S. H.; Poynton, S. D.; Murphy, S.; Ong, A. L.; Varcoe, J. R. *J. Mater. Chem. A* **2013**, *1*, 1018−1021.
(37) Ariese, F.; Kok, S. J.; Verkaik, M.; Hoornweg, G. P.; Gooijer, C.; Velthorst, N. H.; Hofstraat, J. W. *Anal. Chem.* **1993**, *65*, 1100−1106.
(38) Chen, C.; Levitin, G.; Hess, D. W.; Fuller, T. F. *J. Power Sources* **2007**, *169*, 288−295.
(39) Liu, X.; Gao, H.; Chen, X.; Hu, Y.; Pei, S.; Li, H.; Zhang, Y. *J. Membr. Sci.* **2016**, *515*, 268−276.
(40) Salerno, H. L. S.; Elabd, Y. A. *J. Appl. Polym. Sci.* **2013**, *127*, 298−307.
(41) Silverstien, R. M.; Webster, F. X.; Kiemle, D. J. *Spectrometric Idenitfication of Organic Compounds*; 7th ed.; John Wiley & Sons, Inc.: Hoboken, NJ, 2005.
(42) Sanborn, C. D.; Chacko, J.; Ardo, S. *in preparation*.
(43) Hoffmann, E. A.; Fekete, Z. A.; Korugic-karasz, L. S.; Karasz, F. E.; Wilusz, E. *J. Polym. Sci., Part A: Polym. Chem.* **2004**, *42*, 551−556.
(44) Lopez, G. P.; Castner, D. G.; Ratner, B. D. *Surf. Interface Anal.* **1991**, *17*, 267−272.
(45) Schulze, M.; Lorenz, M.; Wagner, N.; Gülzow, E. *Fresenius' J. Anal. Chem.* **1999**, *365*, 106−113.
(46) Chien, H. C.; Tsai, L. D.; Kelarakis, A.; Lai, C. M.; Lin, J. N.; Fang, J.; Zhu, C. Y.; Chang, F. C. *Polymer* **2012**, *53*, 4927−4930.
(47) Haghighat, S.; Ostresh, S.; Dawlaty, J. M. *J. Phys. Chem. B* **2016**, *120*, 1002−1007.
(48) Reiter, R. S.; White, W.; Ardo, S. *J. Electrochem. Soc.* **2016**, *163*, H3132−H3134.
(49) Bard, J. A.; Faulkner, R. L. *Electrochemical Methods: Fundamentals and Applications*; 2nd ed.; John Wiley & Sons, Inc.: New York, 1980.
(50) Shockley, W.; Queisser, H. J. *J. Appl. Phys.* **1961**, *32*, 510−519.
(51) Chang, W. B.; Evans, C. M.; Popere, B. C.; Russ, B. M.; Liu, J.; Newman, J.; Segalman, R. A. *ACS Macro Lett.* **2016**, *5*, 94−98.
(52) Ishida, H.; Tobita, S.; Hasegawa, Y.; Katoh, R.; Nozaki, K. *Coord. Chem. Rev.* **2010**, *254*, 2449−2458.

DOI: 10.1021/jacs.7b00974
J. Am. Chem. Soc. XXXX, XXX, XXX−XXX